Mendeleev Communications

Mendeleev Commun., 2025, **35**, 47–49

Synthetic routes to phosphorus-doped graphene nanoflakes

Evgeniya V. Suslova,*[a] Sergey V. Yakovlev,[b] Konstantin I. Maslakov,[a] Andrey V. Desyatov,[c] Dmitry N. Stolbov,[a] Denis A. Shashurin,[d] Natalia N. Kuznetsova[a] and Serguei V. Savilov[a,b]

[a] *Department of Chemistry, M. V. Lomonosov Moscow State University, 119991 Moscow, Russian Federation. E-mail: suslova@kge.msu.ru*
[b] *N. S. Kurnakov Institute of General and Inorganic Chemistry, Russian Academy of Sciences, 119991 Moscow, Russian Federation*
[c] *D. I. Mendeleev University of Chemical Technology of Russia, 125047 Moscow, Russian Federation*
[d] *Department of Fundamental Medicine, M. V. Lomonosov Moscow State University, 119991 Moscow, Russian Federation*

DOI: 10.71267/mencom.7531

Phosphorous-doped graphene nanoflakes (GNFs) were first synthesized by several methods, including pyrolysis of PPh_3 solution in toluene, post-treatment of GNFs with H_3PO_4 and hydrothermal post-treatment of GNFs or oxidized GNFs with PPh_3 solution in DMF. The products were characterized by scanning and transmission electron microscopy, low-temperature nitrogen physisorption and X-ray photoelectron spectroscopy. Correlations between composition and structural features were revealed.

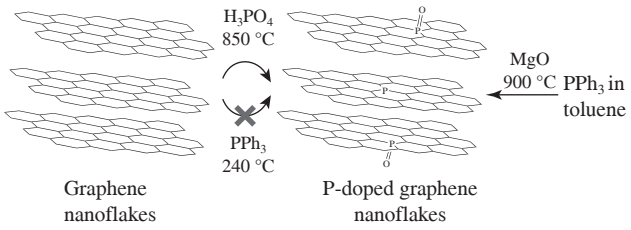

Keywords: phosphorous-doped, graphene nanoflakes, post-doping, porous material, mesopores, X-ray photoelectron spectroscopy.

Phosphorous-doped carbon nanomaterials (CNMs) have a variety of applications. The incorporation of more electronegative phosphorus atoms into graphene layers strongly affects the properties of sp^2 carbon materials, changing their electronic structure[1] and increasing their structural defectiveness.[2] Such phosphorous-doped CNMs can be used as electrode materials for lithium-[3,4] and sodium-ion[5] batteries, as electrocatalysts for oxygen reduction,[6] as well as adsorbents for the removal of imipramine,[7] metal ions and other contaminants[8] from wastewater. They also have a high potential in other areas, for example, as matrices for biomedical contrast agents and drug delivery systems.[9]

Phosphorous-doped CNMs can be produced by pyrolysis of appropriate P-containing precursors or *via* post-doping of a previously synthesized pure carbon structure.[2] For example, P-doped carbon nanotubes (CNTs) were previously synthesized by pyrolysis of PPh_3 in toluene solution,[10] and graphitic nano onion-like structures containing phosphorus and nitrogen atoms were produced by pyrolysis of $FeCp_2$, trioctylphosphine oxide, benzylamine and THF precursors.[11] The post-doping approach was demonstrated in the synthesis of P-doped carbon quantum dots by solvothermal treatment of graphene oxide (GO) with PPh_3 in DMF as solvent,[12] in the preparation of P-doped graphene nanosheets by annealing a mixture of GO and 1-butyl-3-methylimidazolium hexafluorophosphate[13] or in the production of P-doped carbon framework by calcination of phytic acid.[14] It is important to mention the widely used synthesis of P-doped CNMs by treating the carbon material with an aqueous solution of H_3PO_4.[15] This method effectively increases the specific surface area of the material and can be used, for example, to obtain activated carbons from a wide variety of biomass and waste.[16–19]

This work is an extension of the study of different types of carbon nanostructures, which was started almost 20 years ago under the supervision of Academician of the Russian Academy of Sciences Valery V. Lunin. Previously, we reported on the synthesis of undoped,[20] N-doped[21] and N,Si-doped[22] GNFs *via* the decomposition of hexane, acetonitrile or a mixture of tetramethylsilane with acetonitrile, respectively, in the presence of a MgO template, as well as on the modification of the GNFs surface with hydroxyl and carboxyl groups by treatment with HNO_3.[23] In this work, GNFs were synthesized by the pyrolytic decomposition of hexane (for details, see Online Supplementary Materials). We demonstrated that the properties of GNFs and the interaction between graphene layers in their structure depend on the nature and content of heteroatoms.[22] This work is devoted to a systematic study of P-doped GNFs (P-GNFs) synthesized for the first time by four different methods: (i) post-treatment of GNFs with H_3PO_4 at 850 °C, hydrothermal treatment of (ii) pristine and (iii) oxidized GNFs with PPh_3 in DMF solution at 240 °C for 72 h and (iv) pyrolytic decomposition of PPh_3 in toluene solution in the presence of MgO template at 900 °C (Table S1, see Online Supplementary Materials). The physicochemical properties of the obtained materials were analyzed and compared. The characterization methods are described in Online Supplementary Materials. The samples produced by methods (i)–(iv) are denoted as P-GNFs_H_3PO_4, P-GNFs_ht, P-GNFsox_ht and P-GNFs_pyr, respectively.

GNF and P-GNF particles contain 7–10 graphene layers according to transmission electron microscopy (TEM) images (Figure 1), while scanning electron microscopy (SEM) revealed similar sizes of GNF [Figure 2(*a*)] and P-GNF_pyr [Figure 2(*b*)] agglomerates. The nitrogen physisorption isotherms of the obtained materials are a combination of type IVa and type II according to the IUPAC classification [Figure S1(*a*), see Online Supplementary Materials], indicating the contribution of both meso- and macropores. The textural parameters of P-GNFs are summarized in Table 1.

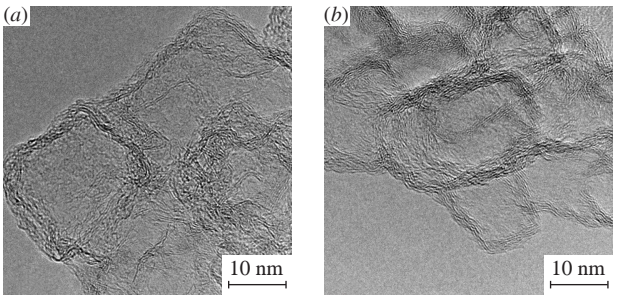

Figure 1 TEM images of (*a*) GNFs and (*b*) P-GNFs_pyr.

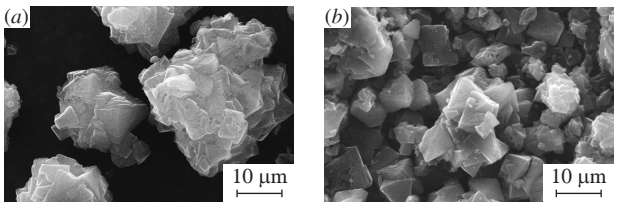

Figure 2 SEM images of (*a*) GNFs and (*b*) P-GNFs_pyr.

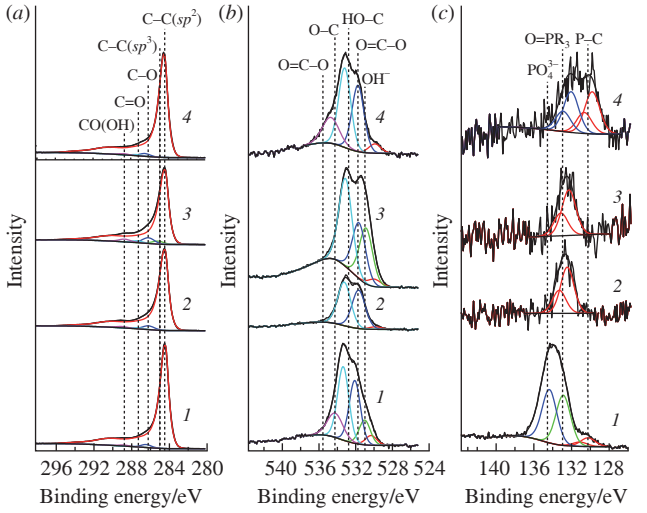

Figure 3 High-resolution XPS spectra of (*a*) C 1*s*, (*b*) O 1*s* and (*c*) P 2*p* of samples (*1*) P-GNFs_H_3PO_4, (*2*) P-GNFs_ht, (*3*) P-GNFsox_ht and (*4*) P-GNFs_pyr.

The calculated BJH mesopore size distributions demonstrate that the narrowest pore size distribution is typical for P-GNFs_H_3PO_4 and P-GNFs_pyr [Figure S1(*b*)]. The phosphorous-containing groups block the pores and reduce S_{BET}.[15] Any treatment of raw GNFs resulted in a decrease of the total pore volume due to an increase of macropores in the structure, while the average pore radius increased (see Table 1).

The content and nature of heteroatoms in the P-GNF samples (see Table 1) were determined by X-ray photoelectron spectroscopy (XPS). The XPS spectra demonstrate C, O and P lines. The C 1*s* XPS spectra were fitted to five components with binding energies of 284.5, 285.2, 286.2, 287.3 and 288.7 eV, corresponding to sp^2- and sp^3-hybridized carbon atoms, C–O, C=O and carboxyl groups, respectively [Figure 3(*a*)]. The analysis of the O 1*s* XPS spectra revealed components at 530.3, 531.2, 532.1 and 533.6 eV, which can be assigned to the O^-, O=C–O, C–OH and O=C–O species [Figure 3(*b*)]. The P content was below 0.4 at% (see Table 1), similar to the reported data for P-doped CNTs[10] and P-doped carbon quantum dots.[12] The P 2*p* XPS spectra were fitted to three components with binding energies of 130.3, 132.8 and 134.4 eV, attributed to P–C, $O{=}PR_3$ and phosphate species [Figure 3(*c*)]. The presence of the P–C component confirms the successful incorporation of P into the carbon layers of P-GNFs_H_3PO_4 and P-GNFs_pyr. The P 2*p* spectra of P-GNFs_ht and P-GNFsox_ht are dominated by the P=O component [see Figure 3(*c*)]. The appearance of $O{=}PPh_3$ bonds in P-GNFs_ht and P-GNFsox_ht can be attributed to the oxidation of PPh_3 or the formation of $O{=}PC_3$ fragments.[13] The defectiveness of the obtained samples can be estimated from the ratio of sp^3- to sp^2-hybridized carbon atoms. The percentage of edge unsaturated sp^3-hybridized atoms increases with increasing oxygen and phosphorus content in the samples (Figure S2).

In summary, we evaluated the synthesis of P-doped GNFs *via* pyrolysis of PPh_3 in toluene, post-treatment of GNFs with H_3PO_4 and hydrothermal post-treatment of GNFs or oxidized GNFs with PPh_3 in DMF solution. The uniform layered structure of GNFs was confirmed by SEM and TEM. However, the efficiency of these methods varied due to the significantly larger size of P atoms compared to C atoms. Another factor increasing the complexity of the synthesis was the affinity of phosphorus atom for oxygen, resulting in the formation of C–P=O fragments. The pyrolysis of PPh_3 resulted in the incorporation of P atoms into the carbon structure, which was confirmed by XPS. The P content was below 0.1 at%, which agrees with the reported data for P-doped CNTs.[10] The treatment of GNFs with H_3PO_4 decreased S_{BET} and pore volume, while the pore radius increased. The final product P-GNFs_H_3PO_4 contains P atoms incorporated into graphene layers and P atoms in the PO_4^{3-} state. The hydrothermal synthesis did not result in the incorporation of P atoms into the GNF structure. Moreover, the amount of oxygen-containing groups after hydrothermal treatment of the P-GNFsox_ht sample decreased significantly (see Table 1), indicating surface defunctionalization. However, S_{BET}, pore volume and pore radius of the products increased. We concluded that the pyrolytic decomposition of a P-containing precursor can be considered the most promising method for the preparation of P-doped GNFs.

This research was funded by the Russian Science Foundation (grant no. 22-15-00072). The authors thank A. P. Kozlov for assistance in the synthesis and S. V. Maximov for obtaining TEM images. The authors acknowledge the support from the MSU Equipment Center 'Nanochemistry and Nanomaterials', operating within the framework of the Lomonosov Moscow State University Program of Development.

Table 1 Textural parameters and XPS composition of GNF and P-GNF materials.

Sample	Specific surface area (S_{BET})/m^2 g^{-1}	Total pore volume/cm^3 g^{-1}	Average pore radius/Å	XPS composition (at%)		
				P	C	O
GNFs	440	1.89	8.8	–	98.1	1.9
GNFsox	400	0.91	3.7	–	90.7	9.3
P-GNFs_H_3PO_4	230	0.83	34.5	0.4	96.9	2.5
P-GNFs_ht	–	–	–	<0.1	97.6	2.3
P-GNFsox_ht	510	1.25	18.8	<0.1	94.4	5.6
P-GNFs_pyr	390	1.00	34.6	<0.1	98.5	1.5

Online Supplementary Materials

Supplementary data associated with this article can be found in the online version at doi: 10.71267/mencom.7531.

References

1 N. Yang, X. Zheng, L. Li, J. Li and Z. Wei, *J. Phys. Chem. C*, 2017, **121**, 19321; https://doi.org/10.1021/acs.jpcc.7b06748.

2 E. Billeter, D. McGlamery, M. Aebli, L. Piveteau, M. V. Kovalenko and N. P. Stadie, *Chem. Mater.*, 2018, **30**, 4580; https://doi.org/10.1021/acs.chemmater.8b00944.

3 G. Moreno-Fernández, M. Granados-Moreno, J. L. Gómez-Urbano and D. Carriazo, *Batteries Supercaps*, 2021, **4**, 469; https://doi.org/10.1002/batt.202000247.

4 H. Zhu, D. Wu, G. Zhang, W. Xu, A. Wang and K. Sun, *Journal of Energy Storage*, 2023, **57**, 106172; https://doi.org/10.1016/j.est.2022.106172.

5 L.-W. Chen, N. Lu, F. Liu, Y. Shao and L. Wang, *Chem. Commun.*, 2024, **60**, 3186; https://doi.org/10.1039/D3CC06080B.

6 X. Zhan, X. Tong, M. Gu, J. Tian, Z. Gao, L. Ma, Y. Xie, Z. Chen, H. Ranganathan, G. Zhang and S. Sun, *Nanomaterials*, 2022, **12**, 1141; https://doi.org/10.3390/nano12071141.

7 W. T. Tee, J. E. Yong, J. Chua, N. Y. L. Loh, B. Y. Z. Hiew, S. Gan and L. Y. Lee, *Sep. Purif. Technol.*, 2024, **330** (C), 125266; https://doi.org/10.1016/j.seppur.2023.125266.

8 L. Feng, Z. Qin, Y. Huang, K. Peng, F. Wang, Y. Yan and Y. Chen, *Sci. Total Environ.*, 2020, **698**, 134239; https://doi.org/10.1016/j.scitotenv.2019.134239.

9 D. A. Shashurin, E. V. Suslova, V. A. Rozhkov, R. V. Sotenskii, O. S. Medvedev and G. A. Shelkov, *Russ. J. Appl. Chem.*, 2023, **96**, 410; https://doi.org/10.1134/S107042722304002X.

10 D. G. Larrude, M. E. H. Maia da Costa, F. H. Monteiro, A. L. Pinto and F. L. Freire, Jr., *J. Appl. Phys.*, 2012, **111**, 064315; https://doi.org/ 10.1063/1.3695452.

11 A. D. Martínez-Iniesta, A. Morelos-Gómez, E. Muñoz-Sandoval and F. López-Urías, *RSC Adv.*, 2021, **11**, 2793; https://doi.org/10.1039/d0ra10019f.

12 S. Yang, C. Zhu, J. Sun, P. He, N. Yuan, J. Ding, G. Ding and X. Xie, *RSC Adv.*, 2015, **5**, 33347; https://doi.org/10.1039/C5RA04001A.

13 R. Li, Z. Wei, X. Gou and W. Xu, *RSC Adv.*, 2013, **3**, 9978; https://doi.org/10.1039/C3RA41079J.

14 X. Zhang, H. Xu, H. Liu, W. Ma, D. Wu, Z. Meng and L. Wang, *Ceram. Int.*, 2024, **50**, 3641; https://doi.org/10.1016/j.ceramint.2023.11.114.

15 Y. Wen, B. Wang, C. Huang, L. Wang and D. Hulicova-Jurcakova, *Chem. – Eur. J.*, 2015, **21**, 80; https://doi.org/10.1002/chem.201404779.

16 Y. Li, X. Zhang, R. Yang, G. Li and C. Hu, *RSC Adv.*, 2015, **5**, 32626; https://doi.org/10.1039/C5RA04634C.

17 T. Budinova, E. Ekinci, F. Yardim, A. Grimm, E. Björnbom, V. Minkova and M. Goranova, *Fuel Process. Technol.*, 2006, **87**, 899; https://doi.org/10.1016/j.fuproc.2006.06.005.

18 W. Astitu, R. A. Hermawan, H. Mukti and N. R. Sugiyono, *AIP Conf. Proc.*, 2017, **1788**, 030082; https://doi.org/10.1063/1.4968335.

19 S. I. Mussatto, M. Fernandes, G. J. M. Rocha, J. J. M. Órfão, J. A. Teixeira and I. C. Roberto, *Bioresour. Technol.*, 2010, **101**, 2450; https://doi.org/10.1016/j.biortech.2009.11.025.

20 S. V. Savilov, N. E. Strokova, A. S. Ivanov, E. A. Arkhipova, A. V. Desyatov, X. Hui, S. M. Aldoshin and V. V. Lunin, *Mater. Res. Bull.*, 2015, **69**, 13; https://doi.org/10.1016/j.materresbull.2015.01.001.

21 S. V. Savilov, E. A. Arkhipova, A. S. Ivanov, K. I. Maslakov, Z. Shen, S. M. Aldoshin and V. V. Lunin, *Mater. Res. Bull.*, 2015, **69**, 7; https://doi.org/10.1016/j.materresbull.2014.12.057.

22 D. N. Stolbov, S. A. Chernyak, K. I. Maslakov, N. N. Kuznetsova and S. V. Savilov, *Russ. Chem. Bull.*, 2022, **71**, 680; https://doi.org/10.1007/s11172-022-3465-7.

23 S. A. Chernyak, A. M. Podgornova, E. A. Arkhipova, R. O. Novotortsev, T. B. Egorova, A. S. Ivanov, K. I. Maslakov, S. V. Savilov and V. V. Lunin, *Appl. Surf. Sci.*, 2018, **439**, 371; https://doi.org/10.1016/j.apsusc.2018.01.059.

Received: 7th June 2024; Com. 24/7531